

# Classification of Nylon 66 Impurities Using Digital Image Processing

CHANDIS R. BRASINGTON and F. GADALA-MARIA\*

Department of Chemical Engineering, University of South Carolina, Columbia, SC 29208

## SYNOPSIS

Color image processing was used to classify the impurities in nylon 66 that fluoresce when exposed to ultraviolet light. The hue value determined from digitized color images was found to correlate well to the color of the fluorescence as seen by the naked eye. Digital image processing is advantageous over visual observation because it removes the subjectivity from the classification process, and is a relatively simple and inexpensive method compared to other spectroscopic techniques. The hue values of the impurities may provide a quantitative data base that could lead to process improvements. © 1994 John Wiley & Sons, Inc.

## INTRODUCTION

During the production of nylon 66, a contaminant (sometimes called gel) forms in the polymer. The molecular structure of the gel and the way in which it is formed are not yet well understood. Filters, called pack screens, are used to remove gel particles and other contaminants from the molten polymer before it enters the spinnerets and is spun into fibers. These pack screens do not capture all of the gel, and the gel that passes through the filters is a major cause of fiber breaks during spinning. The pack screens are periodically removed from the production line and replaced. The screens removed are examined to determine the amount of gel collected in them. The amount of gel that collects on these screens has been correlated to the number of breaks in the fibers during spinning.

Gel particles exhibit fluorescence and phosphorescence in the visible region when exposed to ultraviolet light. It has been observed that to the naked eye there appear to be two different types of gel when pack screens are exposed to ultraviolet light with a wavelength maximum of 366 nm, one type that appears to be a "green" color and one type a "red" color. When the ultraviolet lamps are turned off, phosphorescence is observed more often and with

longer lifetimes from the green gel than from the red gel. Thus the red emission may be caused mostly by fluorescence and the green emission may be mostly due to phosphorescence. It is important to distinguish between the two types of gel particles because quantitative information about each type may help trace the process conditions that favor the formation of each and the effect of each type on the number of fiber breaks. However, detecting color differences visually does not lend itself readily to quantifying the amount of each type of gel on pack screens. We describe here a technique that uses color digital image processing to differentiate between the types of gel that emit light in the visible region by measuring their hue values.

## PREVIOUS WORK

Although the exact molecular structure of the gel has not been determined, some researchers have investigated possible mechanisms for its formation and have studied model compounds that exhibit similar luminescent emissions.<sup>1-5</sup>

### Phosphorescence

In 1974, N. S. Allen et al.<sup>4</sup> studied nylon 66 chips and observed phosphorescence emissions with a maximum at 445 nm when the polymer was excited with ultraviolet light with a wavelength of 365 nm.

\* To whom correspondence should be addressed.

When excited at 300 nm, Allen et al.<sup>6</sup> observed that the phosphorescence emissions from nylon 66 chips had two maxima instead of one, one maximum at 425 nm with a lifetime of 1.6 s and the other at 465 nm with a lifetime 0.6 s. Both maxima were present in film extruded from those chips, but only the maximum at the longer wavelength was observed in fiber spun from the chips, leading them to conclude that the thermal history of the polymer during fiber spinning altered the chemical groups responsible for the phosphorescence emission at the lower wavelength. This is consistent with their finding that the ratio of the intensity of the lower wavelength peak to that of the higher wavelength peak for chips that were thermally oxidized at a constant temperature for a given period of time decreased as the temperature at which the oxidation took place increased. Nylon 66 should not phosphoresce because neither the amide linkage, the carboxylic acid end group, nor the amine end group phosphoresce. Thus, the observed phosphorescence must be due to impurities in the polymer.<sup>6</sup> Allen et al.<sup>6</sup> suggest that the peak at the lower wavelength might be due to ketone linkages and the peak at the higher wavelength might be due to aldehyde end groups.

### Fluorescence

Allen et al.<sup>5</sup> later analyzed nylon 66 in film form and their results indicated that two different chemical substances are responsible for the fluorescence from the polymer. They indicated that one substance produced an emission with a maximum at 326 nm when excited at 290 nm and the other produced an emission with maxima at 390 and 420 nm when excited with light with a maximum intensity at 340 nm. The species that emits at a wavelength peak of 326 nm was extractable from the polymer using 2-propanol, indicating that it was not bound to the polymer. The substance that emits at 390 and 420 nm could not be extracted from the polymer and they concluded that it was bound to the molecular backbone of the polymer. They suggested the latter two emission peaks could be from different compounds because their relative intensities depended on the manufacturing history of the polymer. Scharf et al.<sup>7</sup> identified a structure in nylon 6 that when excited at 340 nm emitted at 420 nm as an  $\alpha$ -ketoimide structure, and Allen et al.<sup>5</sup> concluded that a similar structure may also be present in nylon 66. Dearman et al.<sup>8</sup> found that fluorescence was not observed in nylon 66 monomers indicating that the amide group was not responsible for fluorescence in the polymer and concluded that the fluorescent species in nylon 66 was an impurity.

Previous research has concentrated on phosphorescence and fluorescence emissions in the ultraviolet and near ultraviolet ranges. We are not aware of any work done examining the fluorescence and phosphorescence properties of nylon 66 in the visible range.

## EXPERIMENTAL

### Equipment

A Sony DXC-325 3CCD color camera with a Canon VCL-810BX zoom lens (Sony Corporation, Norcross, GA) connected to Data Translation DT2871 and DT2858 (Data Translation, Marlboro, MA) image processing boards in a Softek 486/33 MHz computer (Softek, Columbia, SC) were used in this project to acquire and manipulate images. Two Blak-Ray XX-15 ultraviolet lamps (Thomas Scientific, Swedesboro, NJ) that emit ultraviolet radiation at a maximum wavelength of 366 nm were used to irradiate the samples. Figure 1 is a schematic of the equipment used in this research. The camera was held vertically above the sample in a Kaiser RSX-5512 copy stand (Kaiser, Germany) and the tip of the lens was 7.6 cm above the base. The camera was set on a gain of 0 dB, with the iris open at F 1.4. The lamps were held in stands with the bottom point of the lamps placed 37.0 cm apart and 3.9 cm above the copy stand base. The lamps were placed at an angle of 64° from the horizontal and were controlled by an input/output card in the computer. The ultraviolet lamps were found to have a "charging" time; the output from the ultraviolet lamps followed a trend similar to a second order response to a step input (turning on the lights). The ultraviolet lamps exhibited this behavior independent of whether they were connected to the input/output card in the computer or directly to the wall outlet. The time required for the lights to settle close to equilibrium was approximately 3000 s. For this reason, the ultraviolet lights were allowed to equilibrate for at least 1 h before experiments were performed.

The image boards used in our research digitize the incoming analog red, green, and blue (RGB) video signals from the color camera to form a color image made of 512 columns by 480 rows of individual pixels. Light entering the camera lens is divided into the red, green, and blue portions of the spectrum by a prism, with each portion reaching a different CCD chip. The sensors on each chip measure the energy of the photons that reach it and send a corresponding signal to the digitizing board. The board converts each of the red, green, and blue signals to values

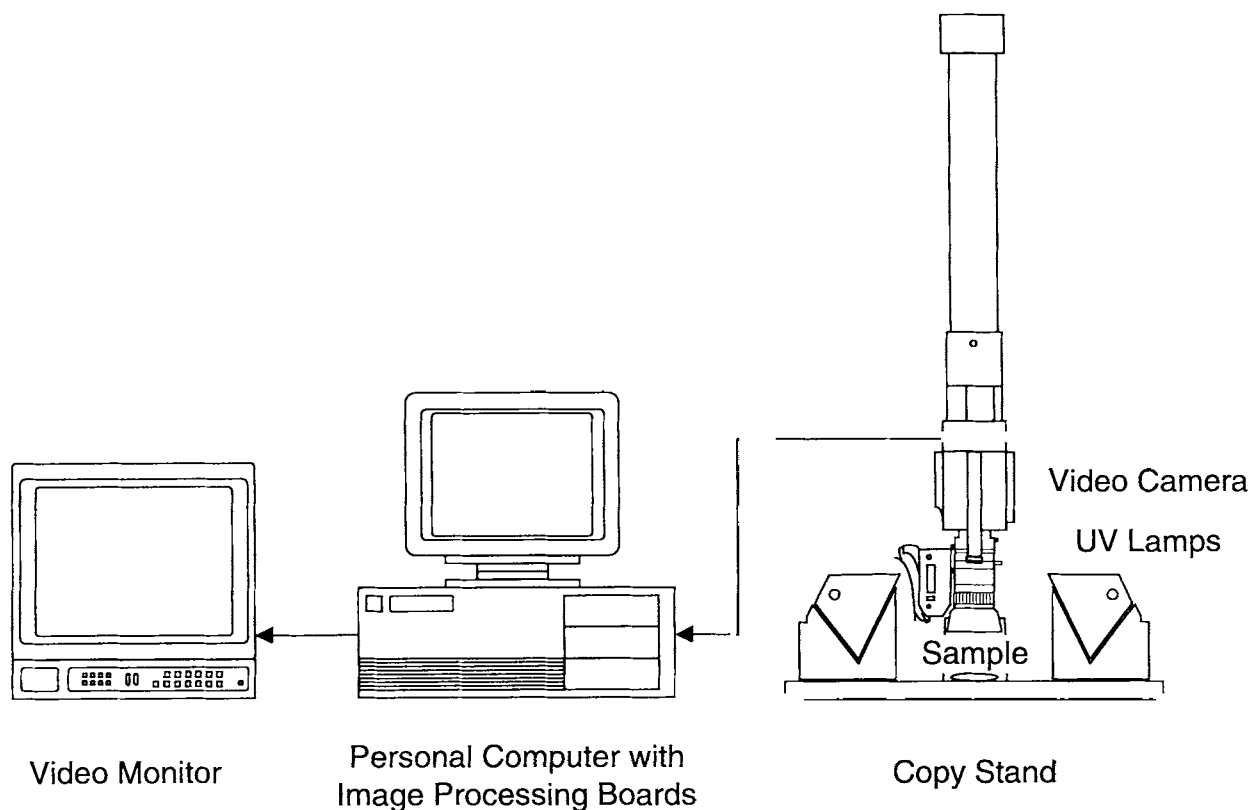


Figure 1 Equipment configuration.

ranging from 0 to 255. This particular board is able to convert the RGB information to HSI (hue, saturation, intensity) values as the data is being acquired. Conversion of RGB to HSI occurs via the equations presented below.<sup>9</sup> Intensity is calculated by

The hue is calculated by

$$H = 255(1/360^\circ)[90^\circ - \arctan(F/\sqrt{3})]$$

$$S = 255\{1 - [\min(R, G, B)/I]\}.$$

Figure 2 is a geometric representation of the method used to convert RGB values to HSI values.<sup>9</sup> The intensity is the average of the red, green, and blue signals and is equivalent to the gray level obtained when a black-and-white image is digitized. At a given

intensity level, the red, green, and blue values are plotted on a triangular diagram. Every point in that triangular diagram represents a combination of red, green, and blue with the same intensity. The point in the center of the triangular diagram, where the values of red, green, and blue are equal, represents a level of gray somewhere between black and white. This point has a saturation value of zero. The points at the edges of the triangle represent pixels with a maximum saturation (not diluted with white). The saturation of a given point in the triangle is calculated as the ratio of the length of the line from the center to the given point to the length of the line from the center to the edge of the triangle that passes through that point. The hue value is calculated from the angle between the line connecting the center to the red corner and the line connecting the center to the point of interest. All points at a given angle have the same hue. The angles, which vary from 0 to 360°, are normalized to vary from 0 to 255. Moving counterclockwise, hues vary from red (0) to orange (17) to yellow (40) to green (85) to blue (170) to purple (200) and then back to red again (255). In this research, hue is the parameter that is used to distinguish the different luminescent emissions of gel.

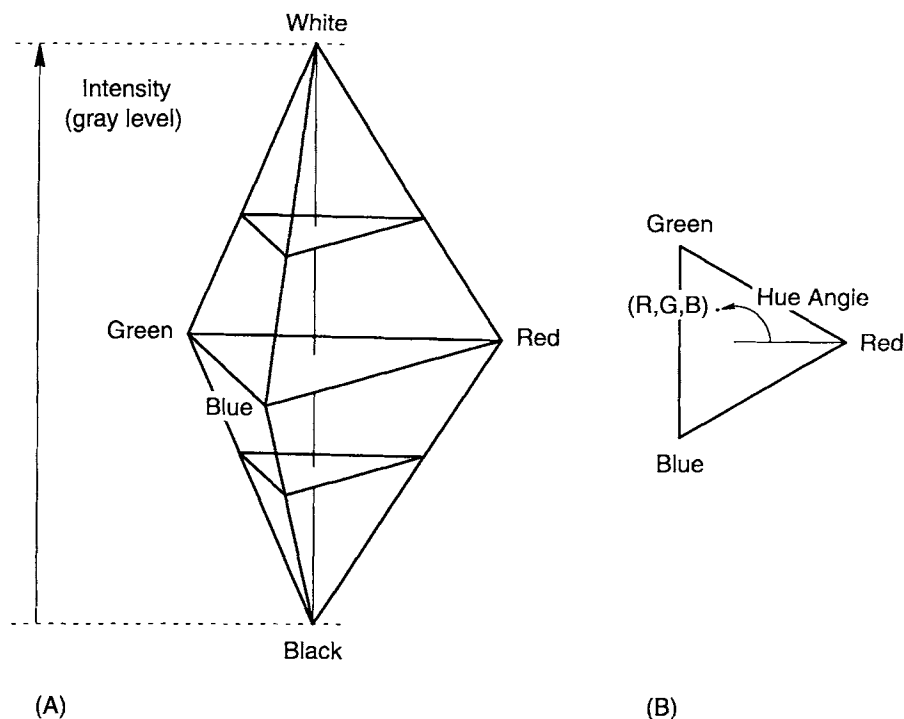


**Figure 2** The HSI (hue, saturation, intensity) triangle model. (A) Three-dimensional view showing the intensity axis. (B) Cross-sectional view showing the hue angle.

### Preliminary Measurements

In order to examine the reproducibility of hue values, some preliminary experiments were performed. After the lights had equilibrated, a pack screen was placed under the ultraviolet lights and viewed using the camera. The gel particles were exposed to the ultraviolet light for 10 s before the first image was acquired. Four more images were acquired at 10-s intervals. Each image was digitized in HSI format and saved to the hard drive of the computer before the next image was acquired.

The first image acquired was retrieved from the hard drive and displayed on the video monitor. Gel particles appeared almost round in the images and a rectangular area inside each gel particle was chosen for analysis. The analysis area was chosen by the user by moving a cursor across the image and marking the upper left corner and the lower right corner of the desired area of analysis. The average hue for the gel particle was calculated by summing the hue value of each pixel and dividing by the number of pixels examined. The same area of analysis and the same calculations were performed on the other four images. All five average hue values were themselves averaged to give an overall average hue for each gel particle. The color emitted from each gel particle as seen by the naked eye was also recorded. Experi-

ments were performed at 69°F in air at atmospheric pressure.

Examining the average hue values for the five images taken of each gel particle, it was evident that over a short period of exposure to ultraviolet light (approximately 1 min), the hue values were relatively constant. For the gel particles analyzed, the average hue values were consistent to  $\pm 0.5$  on a scale from 0 to 255. Because of the reproducibility of hue values in the preliminary measurements, only one image was acquired in subsequent measurements.

### Subsequent Measurements

The average hue value of a gel particle was determined from the digitized image as follows. The hue values of all the pixels representing the particle were measured by moving a cursor to each of those pixels and recording its hue value. A pixel was considered part of a gel particle if its intensity value was significantly larger than intensity values of the background. The hue values collected were averaged for each gel particle. Again, the color of luminescence emission from each gel particle as seen by the naked eye was recorded.

In this research, 135 gel particles from 24 pack screens were analyzed. The average hues of gel par-

ticles that fluoresce red and for gel particles that fluoresce green as seen by the naked eye are shown on a histogram in Figure 3. This figure demonstrates that the red and green gel particles can be distinguished by their hue values as determined through image processing. A slight overlap in the data for red and green gel particles is evident in Figure 3, which indicates that in the region around a hue of 150 it is difficult to distinguish the two chromophores. The hue values for gel particles that fluoresce a green color cover a wider range of hue values than for gel that fluoresces a red color. From Figure 3, it is apparent that the mean hue value for each of the two types of gel particles is different. A significant difference in means for red and green gel particles was confirmed at an  $\alpha$  of 0.05 using a Tukey test. The mean hue value for green gel was 139.6 with a standard deviation of 6.4. The mean hue value for red gel was 156.1 with a standard deviation of 3.0.

Gel particles from one set of two pack screens removed from the same machine on the same day were analyzed. A total of 25 gel particles composed of 69 pixels were analyzed. Figure 4 is a histogram of the average hue values of the gel particles from this set of pack screens (one value per particle) and Figure 5 is a histogram of the hue values of the individual pixels of these gel particles (one value per pixel). The histograms are similar to that shown in Figure 3 for all particles analyzed. It is clear that this method of distinguishing the different types of gel on pack screens is feasible and could be implemented in existing image processing systems to provide quantitative information about different types of gels that could lead to process improvements.

### SOURCES OF ERROR

The average hue values of both types of gel particles are skewed toward the blue, possibly because the ultraviolet lamps also emit blue light.

The hue value was found to decrease slightly (by one or two units) when the distance between the ultraviolet lamps and the gel particles was increased about 10%. This is due to the decrease in the blue value in the RGB mode. At the distance used, the blue component remained close to its maximum value of 255 for all pixels.

Depending on how well the pack screens are cleaned when they are removed, there may be a layer of polymer covering the gel particles. The hue of a gel particle covered in polymer is approximately one average hue value lower than for the gel particle without polymer cover. This is only a slight shift in the hue value and can be regarded as a negligible influence on hue.

Tests were also performed to determine if long-term exposure to ultraviolet light affected the hue of gel particles and the results showed that after 5.5 h of exposure to ultraviolet light, the hue increased about one hue unit on the average. This increase in hue is an indication of a slight decrease in emission wavelength with increased exposure to ultraviolet light. (Allen et al.<sup>6</sup> observed a slight decrease in phosphorescence emission wavelength during photooxidation experiments.)

If a different system for analysis of gel particles were used, such as a different camera and lens, or different image processing boards, the ranges for the

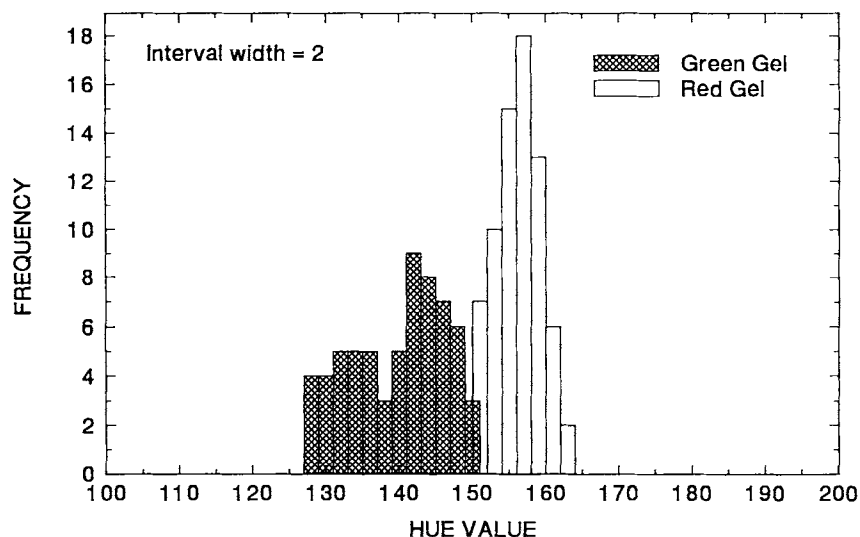


Figure 3 Hue distribution of all gel particles examined.

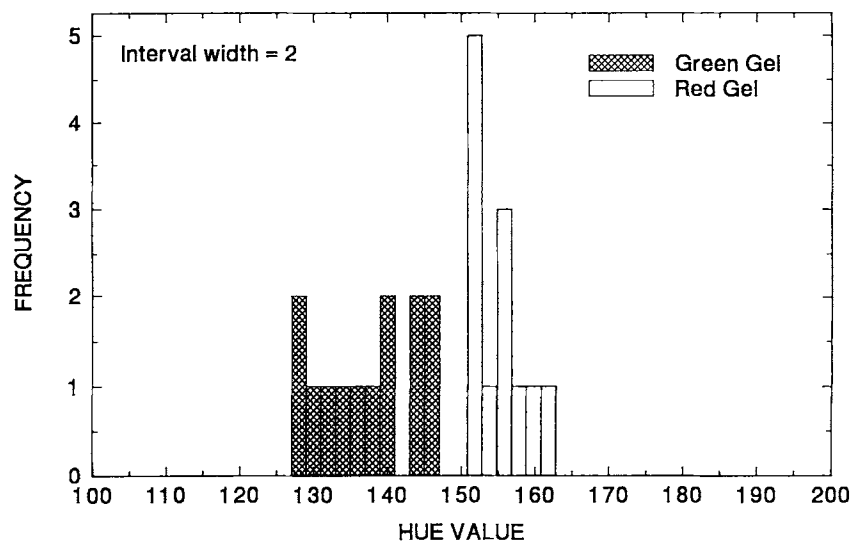


Figure 4 Hue distribution of the gel particles on one set of pack screens.

hue values of red gel particles and green gel particles might be slightly different. A different digital image processing system of equal or better quality, though, should still be able to detect the hue differences between the two types of gel.

### CONCLUSIONS AND RECOMMENDATIONS

Two types of gel in nylon 66, gel that appears a red color and gel that appears a green color to the naked eye, can be distinguished by their difference in hue

values as detected by a camera and image processing boards. A limitation of image processing is that the wavelength spectra of the emissions cannot be determined. Nonetheless, the fact that different hue values are detected for the two gel types indicates that they have different wavelength emission spectra. The absorption of ultraviolet light occurs at the same energy level for both gel types and the emission of visible light occurs at different wavelengths for the two gel types, suggesting that each type of gel is excited to a different energy level. Because green gel has lower hue values than red gel, luminescence emission occurs at longer wavelengths (lower en-

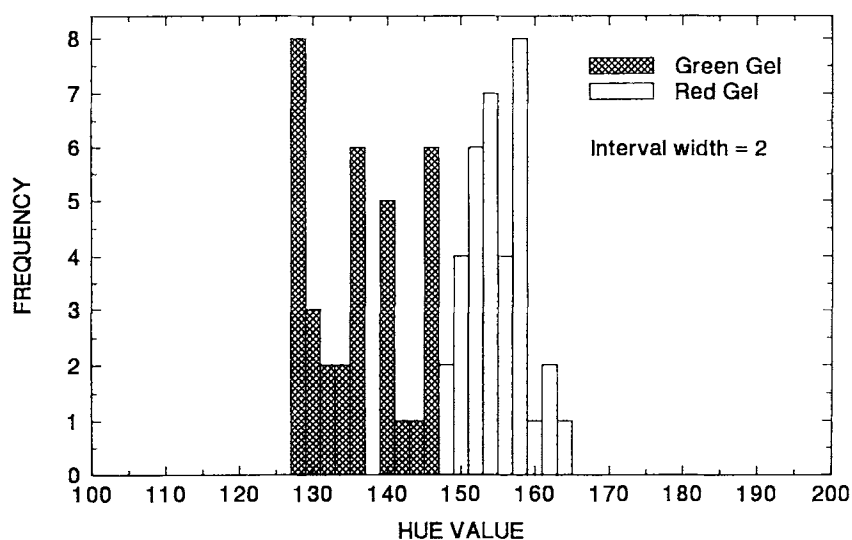


Figure 5 Hue distribution of the pixels representing the gel particles on one set of pack screens.

ergy) for green gel than for red gel. It is possible that the lower energy level for emission from green gel occurs from a triplet state (phosphorescence) and the higher energy level for luminescence emission from red gel occurs from a singlet state (fluorescence). Further research should be done to investigate this possibility. The results suggest that the molecular structure responsible for the luminescence of the two types of gel are different because the emission spectra are different.

Examining Figure 3, it is evident that there is not a clear break between the two colors of gel. It is possible that some type of progression from one gel type to another occurs by way of the extent of thermally oxidative degradation of the polymer as suggested by Allen et al.<sup>6</sup> It is possible that the emission spectrum of a gel particle is a combination of the emission spectra of several types of luminescent structures.

The information acquired from the present research could be used to improve existing image processing techniques for examining gel particles. Not only could the size and area of all gel particles be measured, but the data could be divided into two categories by their average hue values. Additional quantitative information about each type of gel could aid in tracing problems in the production of nylon 66 by linking the amounts of each type of gel to the number of fiber breaks during fiber spinning. Using image processing to analyze different types of gel is an advantageous method because the method of analysis is simple as compared to other spectroscopic techniques where samples are dissolved in a solvent or extruded into a thin film for analysis. In addition,

image processing produces more quantitative information than the subjective method of visually differentiating the gel types.

We would like to express our gratitude to E. I. du Pont de Nemours and Company for providing the financial support for this research and the samples for analysis. A special thanks goes to Ray Amyette of Du Pont's May Plant for his help with this project.

## REFERENCES

1. D. D. Steppan, M. F. Doherty, and M. F. Malone, *J. Appl. Polym. Sci.*, **42**, 1009 (1990).
2. L. H. Peebles, Jr. and M. W. Huffman, *J. Polym. Sci. A-1*, **9**, 1807 (1971).
3. H. A. Taylor, W. C. Tincher, and W. F. Hamner, *J. Appl. Polym. Sci.*, **14**, 141 (1970).
4. N. S. Allen, J. F. McKellar, and G. O. Phillips, *J. Polym. Sci., Polym. Chem.*, **12**, 2623 (1974).
5. N. S. Allen and M. J. Harrison, *Eur. Polym. J.*, **21**, 517 (1985).
6. N. S. Allen, J. F. McKellar, and G. O. Phillips, *J. Polym. Sci., Polym. Chem.*, **12**, 1233 (1974).
7. H. D. Scharf, C. D. Dieris, and H. Leismann, *Angew. Makromolek. Chem.*, **79**, 193 (1979).
8. H. H. Dearman, F. T. Lang, and W. C. Neely, *J. Polym. Sci. A-2*, **7**, 497 (1969).
9. S. E. Genz, *Real Time Chip Set Simplifies Color Image Processing*, Data Translation, Inc. New Products Handbook, 1984.

Received November 8, 1993

Accepted February 5, 1994